Recent advances in layered double hydroxides-based electrochemical sensors: Insight in transition metal contribution

Christine Mousty, Hani Farhat

Recent advances in layered double hydroxides-based electrochemical sensors: insight in transition metal contribution

Christine MOUSTY and Hani FARHAT*

[a] Université Clermont Auvergne, CNRS, Institut de Chimie de Clermont-Ferrand (ICCF), F-63000 Clermont-Ferrand, France.
* e-mail: Christine.Mousty@uca.fr

Received: 1 December 2022
Accepted: 13 January 2023

Abstract
Among the nanomaterials reported in the literature, layered double hydroxides (LDHs) are considered promising for the electrochemical sensor technology. Transition metal-based layered double hydroxides (TM-LDHs) show excellent electrocatalytic properties that facilitate redox reactions with analytes, e.g. H_2O_2, glucose or glyphosate. Elaboration of porous nano-structures with TM-LDHs nanosheets on the electrode surface allows a rapid diffusion of the analytes and a good accessibility of the TM active sites. An association of TM-LDHs with conductive materials, e.g. graphene or metal nanoparticles (M-NPs), improves the electronic conductivity in the LDH-based composites and also the electrocatalytic activity. With a selection of recent publications, the present mini-review aims to discuss about the specific electrocatalytic role played by TMs (Ni, Co, Cu, Mn and Fe) present in the LDH layers on the performance (sensitivity and detection limit) of these TM-LDHs-based sensors.

Keywords: Layered double hydroxides, Transition metals, Electrochemical sensors, Hydrogen peroxide, glucose, glyphosate.

DOI: 10.1002/elan.202200527

1. Introduction

In the wide range of electrochemical sensors and biosensors described in the literature, inorganic or hybrid materials, such as silica-based materials [1], cationic clays [2], anionic clays called layered double hydroxides (LDHs) [2c, 3] or metal organic frameworks (MOFs) [4], has been chosen as electrode modifiers for their capacity to accumulate analyte molecules or to immobilize redox mediators and biocatalysts (i.e. hemoproteins, enzymes, bacteria). Moreover, these materials may have their own electrocatalytic properties that can be implied in a transducing process. To improve the performance of these electrochemical sensors, a nano-structuration of these materials on the electrode surface can be realized to increase the electroactive interface between the analyte solution and the electrode transducer, facilitating the diffusional pathway or an efficient electron transfer [5]. Two dimensional (2D) compounds, like LDHs, have a prominent place in these approaches [6].

LDHs, also known as hydrotalcite-like compounds with reference to the natural occurring mineral hydrotalcite $Mg_6Al_2(OH)_6$-CO_3.$4H_2O$, are a versatile class of lamellar compounds. Unlike cationic clays which are in majority natural minerals, LDHs are mostly synthesized compounds. The structure of the LDH layer is similar to that of brucite, with edge-sharing metal-hydroxide octahedra $M(OH)_6$ in which the partial substitution of divalent metal (M^{2+}) by trivalent metal (M^{3+}) cations induces positively charged layers balanced by intercalated exchangeable anions (Fig.1). The LDH general formula is $[M^{2+}_{1-x}M^{3+}_x(OH)_2]^{x+}A^{n-}_{x/n}.yH_2O$, abbreviated $M^{2+}M^{3+}$-A, where M^{2+} and M^{3+} are divalent and trivalent metal cations, respectively, and A^{n-} represents a *n*-valent anion. The main interest in LDHs is founded on the availability of a large range of compositions for both the metal cations in the hydroxide layers and the interlayer anions [7]. The (MgAl, ZnAl) couples in LDH layers have been the most widely studied, but these cations can be replaced by many others, in particular by transition metals such as Co, Ni, Cu

as divalent cations and Cr, Co, Fe, Mn as trivalent cations. Similarly, the interlayer anions can be substituted by a great variety of inorganic and organic anions or metal complexes, for instance electroactive anions, such as, ferrocene derivatives, 2,2'-azino-bis (3-ethylbenzthiazoline-6-sulfonate) (ABTS), metal porphyrins (FeTSPP), metal phtalocyanines, ferrocyanide ($Fe(CN)_6^{3-}$), etc. [7-8]. Remarkably, all these LDHs can be readily prepared through simple synthesis methods, like coprecipitation at controlled pH or electrodeposition, enabling their composition and morphology to be tuned at the nano-scale. Moreover, carboneous materials [9], e.g. graphene (G), reduced graphene oxide (RGO), multiwall carbon nanotubes (MWCNTs), or metal nanoparticles (M-NPs) [10] can be associated with the LDHs that allows to deeply modulate the specific properties of the resulting nano-composite materials, for instance their electrical conductivity.

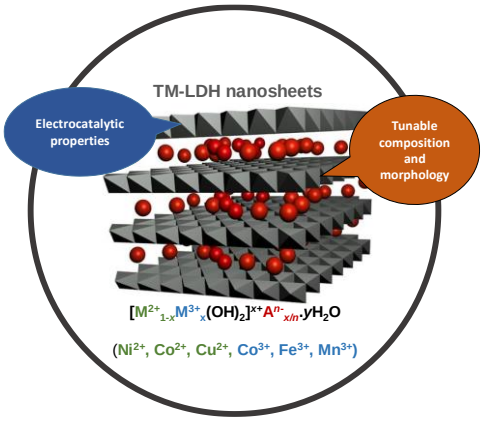

Fig. 1. Scheme of TM-LDHs structure and composition

All these approaches confer to TM-LDHs and hybrid LDHs very interesting electrochemical properties that find applications in various domains. Indeed, LDHs have been used as electrode materials for at least two decades (Fig.2), as evidenced by the abundant literature described in review articles published in the last two years. LDH-based electrodes are used to energy storage as supercapacitors[11], to electrocatalysis for oxygen evolution reaction (OER) and hydrogen evolution reaction (HER)[12] and also in electroanalysis with the design of sensors and biosensors[3, 8, 13] for the quantification of small biomarkers[14], emerging pharmaceutical compounds [15], pesticides [16] or heavy metals [17]. Among all these sensing devices, TM-based LDHs seem to play a key role with their own electrocatalytic properties towards some analyte molecules, such as H_2O_2, glucose and glyphosate. With a selection of recent publications, the present mini-review aims to discuss about the specific electrocatalytic role played by TMs (Ni, Co, Cu, Mn and Fe) present in the LDH layers. The analytical characteristics, namely the sensitivity (S) and the limit of detection (LoD), are scrutinized in relation with the composition and the morphology of TM-LDH modified electrodes.

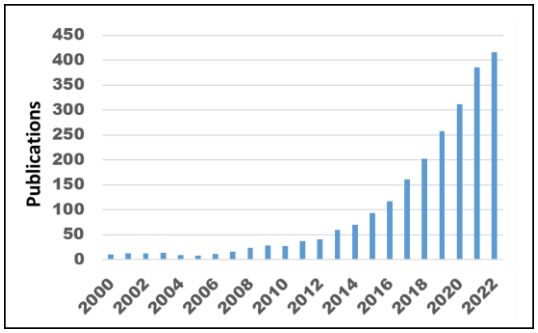

Fig. 2. Number of publications dealing with "LDH and electrodes" published between 2000 and 2022 (data extracted from Web Science)

These reported TM-LDH sensors are mainly prepared as thin films casted on the working electrode surface (glassy carbon electrode (GCE), platinum (Pt), indium tin oxide (ITO), carbon cloth (CC), copper foam (CuF), etc.) or as a component in carbon paste electrodes (CPE). Different ways to prepare LDH films are described. The most popular method corresponds to a "two-step method" in which a LDH colloidal suspension is first prepared and then coated on the electrode surface by means of solvent casting. In some cases, additives, e.g. Nafion, may be added to improve the mechanical stability. *In situ* growth of LDH particles on a conductive support, such as CC, can be achieved during a hydrothermal treatment in the presence of metal salts and support. Finally, LDH thin films can be electrogenerated directly at the electrode surface thanks to the nitrate reduction under potentiostatic or galvanostic conditions. The electrogenerated hydroxide anions are used as precipitant agent of the mixed metal salts to form LDH at the electrode surface. More sophisticated methods to build 3D nano-architectures will be described in details below. The transduction measurements are performed by chronoamperometry at a fixed applied potential (E^{app}). The reference electrode is generally a saturated calomel electrode (E°SCE = 0.242 V) or a silver-silver chloride electrode (E°Ag-AgCl/KClsat = 0.197 V). In alkaline environment, a Hg/HgO reference electrode can replace these reference electrodes (E°Hg/HgO = 0.098 V).

2. H_2O_2 detection

Due to the significance of hydrogen peroxide (H_2O_2) in biomedical or industrial processes, e.g. pharmaceutical, textile and food manufacturing, the development of efficient electrochemical H_2O_2 sensors holds a special attention of researchers [18]. In addition to electrochemical biosensors developed from the immobilization of proteins, such as hemoglobin (Hb) and horse radish peroxidase (HRP) in LDH host matrices [7], other hybrid LDHs containing redox meditators [3b], i.e. ZnCr-FeTSPP or MgAl-$Fe(CN)_6$, have been used to develop electrochemical sensors for H_2O_2 detection. Recently, new sensors have been described in the literature using LDH containing transition metals in their layer structure.

Intrinsic peroxidase-like activity of TM-LDHs, i.e. NiAl [19], CoAl [20], NiCo [21], NiFe [22], CoFe [23], has been reported in the literature. In the presence of H_2O_2, the oxidation of typical peroxidase substrates, such as ABTS or luminol, was catalyzed by these TM-LDHs, leading to a change in the UV-Vis absorbance spectra. Exfoliated LDH phases or 3D hierarchically porous structure exhibited higher catalytic activity due to a better accessibility of active sites than in pristine bulky LDH colloidal suspensions [20]. In comparison to these colorimetric methods, which are time and reactant consuming, the electroanalytical methods offer rapid and sensitive responses. For most TM-LDHs based electrochemical sensors, the transduction reaction consists in the electrocatalytic oxidation of H_2O_2 in alkaline medium (pH 13) (Table 1). Some examples, shown in this table, correspond to the reduction of H_2O_2 in neutral pH solution.

Yin et al. [24] were the first to compare two different H_2O_2 sensors based on NiAl-NO_3 and CoAl-NO_3 LDH. These modified electrodes were prepared by the electrochemical deposition method. The electrochemical signal of CoAl-NO_3, recorded by cyclic voltammetry (CV) in 0.1 M NaOH, is different to the NiAl-NO_3 CV signal. The peaks of the reversible redox couple Co^{II}/Co^{III}, which are broader, are situated at lower potentials ($E_{1/2} \approx 0.46$ V/Ag-AgCl) in respect to the couple Ni^{II}/Ni^{III} ($E_{1/2} \approx 0.60$ V/Ag-AgCl). The electrochemical response of NiAl-NO_3 shows that the electrochemical reaction is governed by a diffusional process. Electron hopping between immobile Ni redox centers and diffusion of both anions and cations throughout the solid lead to a progressive growing of the reaction zone [25]. Whereas in the case of CoAl-NO_3/GCE, the electron transfer seems to be faster and mainly confined at the outer surface of Co_2Al-NO_3 film with an accumulation of ions at the solid/electrolyte interface [25b]. This means that this later faradic process regarding its surface component may be defined more like a pseudocapacitive behavior.

For both types of LDHs, the CV shows an increase of the anodic current after addition of H_2O_2 but at 0.49 V for CoAl-NO_3 and at 0.06 V/Ag-AgCl for NiAl-NO_3, very far from the Ni^{II}/Ni^{III} redox potential. Considering this difference in applied potential (E^{app}), one can consider that the mechanisms of H_2O_2 oxidation are different. The authors propose that H_2O_2 participated to a redox reaction with CoAl-NO_3, whereas NiAl-NO_3 would facilitate the direct oxidation of H_2O_2 with the generation of O_2 [24]. Compared to CoAl-NO_3/GCE, the sensor NiAl-NO_3/GCE showed lower detection limit (LoD) (Table 1) and better reproducibility. Interestingly, the substitution of Al^{III} by Fe^{III} in nickel-based LDH causes a shift of the Ni redox signal towards less anodic potential ($E_{1/2} \approx 0.35$ V/SCE) [25a]. NiFe-LDH nanosheets were formed on Ni foam (NiF) through a facile one-step hydrothermal approach [26]. This NiFe-LDH/NiF electrode exhibited remarkable electrocatalytic activity towards H_2O_2 oxidation at 0.4 V/SCE with a reported sensitivity of 1.7 A M^{-1} cm^{-2}. This impressive performance suggests the existence of a synergistic effect between nickel and iron cations in the LDH nanosheets to enhance the electrocatalytic activity towards H_2O_2 oxidation.

A nanocomposite based on CoAl-CO_3 and MWCNTs was used in a carbon paste electrode (CPE) [27]. The electrochemical response of Co^{II}/Co^{III} in 1 M NaOH was enhanced using the composite MWCNTs@CoAl-CO_3 CPE in place of CoAl-CO_2 CPE, due to the presence of the conductive MWCNTs. H_2O_2 electro-oxidation was processed by active Co species at slightly lower potential than the previously described CoAl-NO_3/GCE sensor (Table 1). The proposed mechanism involving Co species is the following:

$$Co^{II}\text{-LDH} + OH^- \rightleftharpoons Co^{III}(OH)\text{-LDH} + 1e^- \quad (1)$$

$$2Co^{III}(OH)\text{-LDH} + H_2O_2 \rightleftharpoons 2Co^{II}\text{-LDH} + O_2 + 2H_2O \quad (2)$$

An electroreduction of H_2O_2 occurred simultaneously at -0.35 V/Ag-AgCl by an enhanced direct electron transfer promoted by conductive MWCNTs.

Due to the combination of mixed valence states of cobalt and manganese, CoMn-CO_3 has demonstrated interesting electrochemical properties for H_2O_2 oxidation [28]. Indeed, the CoMn-CO_3/GCE is effective in neutral pH compared to other CoAl and NiAl LDH based sensors which must be used in basic solution (Table 1). This distinctive property arises from a synergistic electronic coupling between mixed-valent Co(II)/Co(III) and Mn(III) cations, hosted jointly in the octahedral sites of the LDH structure. Xu et al. [29] have also mentioned the use of CoMn-NO_3 combined with gold nanoparticles (AuNPs) for H_2O_2 electrodetection in neutral pH solution. To explore the action of CoMn-CO_3 as a support for AuNPs, single TM-LDHs (CoAl-CO_3 and MgMn-CO_3) were also tested (Table 1).

Table 1 Electrochemical sensing of H_2O_2 using TM-LDH modified electrodes

LDH	Sensing conditions	Sensitivity ($mA\ M^{-1}\ cm^{-2}$)	LoD (M)	Ref
	H_2O_2 oxidation			
NiAl-NO_3	E^{app} = 0.06V/Ag-AgCl pH 13	-	$9x10^{-9}$	[24]
CoAl-NO_3	E^{app} = 0.49 V/Ag-AgCl pH 13	-	$5x10^{-8}$	
NiFe-NO_3	E^{app} = 0.40 V/SCE pH 13	1704	$5x10^{-7}$	[26]
MWCNTs@CoAl-CO_3	E^{app} = 0.23 V/Ag-AgCl pH 14	118	$5x10^{-6}$	[27]
CoMn-CO_3	E^{app} = 0.65 V/SCE pH 7.0	30	$8.6x10^{-5}$	[28]
AuNPs@CoAl-CO_3		60	$1x10^{-7}$	
AuNPs@MgMn-CO_3	E^{app} = 0.55 V/Ag-AgCl pH 7.0	23	$2.5x10^{-7}$	[29]
AuNPs@CoMn-CO_3		125	$6x10^{-8}$	
	H_2O_2 reduction			
CoCo-NO_3	E^{app} = -0.45 V/SCE pH 7.4	272	$2x10^{-6}$	[30]
AgNPs@NiAl-NO_3	E^{app} = -0.9 V/Ag-AgCl pH 7.0	1.8	$1x10^{-6}$	[31]
AgNPs/PPy@NiAl-CO_3	E^{app} = -0.3 V/SCE pH 7.0	257	$2.8x10^{-7}$	[32]
Fe_3O_4NS@CuAl-CO_3	E^{app} = -0.7 V/ ? pH 7.4	-	$1x10^{-9}$	[33]

A good dispersion of small-sized AuNPs was observed on CoMn-CO_3. The resulting AuNPs@CoMn-CO_3 nanocomposite was successfully applied to H_2O_2 detection in neutral pH with the combine electrocatalytic actions of AuNPs and CoMn-NO_3, leading to a better sensitivity compared to the other composites, AuNPs@CoAl-CO_3 and AuNPs@MgMn-CO_3 or CoMn-CO_3 alone (Table 1).

Tuning the morphology of the catalyst surface with a three dimensional architecture has demonstrated as an effective strategy to improve the catalytic performances of nano-catalysts. For instance, a monometallic $Co^{II}Co^{III}$-NO_3 LDH was prepared by a solvothermal reaction. The catalytic performance of $Co^{II}Co^{III}$-NO_3 was governed by the Co^{II}/Co^{III} ratio which could be simply regulated by tuning the solvothermal reaction time and the three-dimensional flowerlike architecture with abundant accessible active sites [30]. The $Co^{II}Co^{III}$-NO_3/GCE with a high atomic Co^{II}/Co^{III} ratio of 2.34 was reported as good sensor for H_2O_2 (Table 1). Noticeably in this case, H_2O_2 detection proceeds in neutral pH through an absorption-reduction process at -0.45 V/SCE.

Interestingly, Habibi et al. [31] have compared the electrochemical performance of a NiAl-NO_3 CPE with another CPE containing a AgNPs@NiAl-NO_3 composite. It was found that NiAl-NO_3 modified CPE exhibits a weak response at -0.9 V/Ag-AgCl after the addition of H_2O_2 in 0.1 M phosphate buffer solution (PBS, pH 7). The same observation was done with a polypyrrole (PPy)@NiAl-LDH composite (see below). However, the presence of silver nanoparticles (AgNPs) anchored on the LDH particles provides an enhanced electrocatalytic activity with a sensitivity multiplied by eight (Table 1). This strategy was very recently improved using AgNPs anchored on a PPy@NiAl-LDH composite [32]. This latter sensor exhibited an excellent sensing performance towards H_2O_2 with a high sensitivity (257 $mA\ M^{-1}\cdot cm^{-2}$) and a low detection limit of 0.28 µM, measured at a less cathodic potential (E^{app} = -0.3 V/SCE) (Table 1).

Finally, a multifunctional core-shell nanomaterial based on the integration of CuAl-CO_3 LDH over the surface of iron oxide (Fe_3O_4) nanospheres (NS) (Fig.3) was also explored for the sensitive detection of H_2O_2 in PBS pH 7.4 at -0.7 V (Table 1) [33]. The as-prepared Fe_3O_4NS@CuAl-CO_3/GCE composite electrode exhibits an enhanced reduction current density at lower over-potential as compared to CuAl-NO_3/GCE. A synergistic effect is proposed to arise for the electron transfer at the nanoscale interface between Fe_3O_4NS and CuAl-CO_3 LDH,

enhancing the catalytic activity of the Fe_3O_4Ns@CuAl-CO_3/GCE which has been used for *in vitro* determination. of H_2O_2 concentrations in human urine and serum samples.

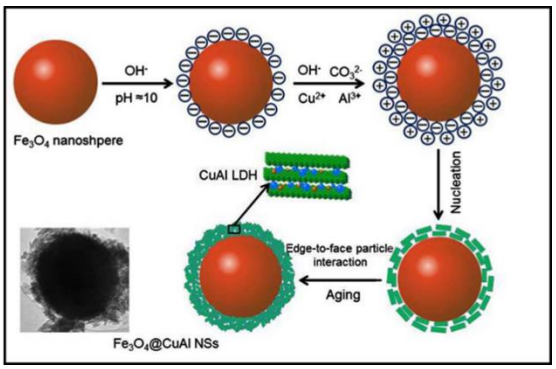

Fig. 3. Scheme of elaboration process of the Fe_3O_4Ns@CuAl-CO_3, Reprinted from [33] with permission from Elsevier.

All these examples show that H_2O_2 can be detected by its electrocatalytic oxidation with Ni or Co based LDH. However in reduction, the electrocatalytic process can be attributed mainly to the presence of AgNPs immobilized on LDH particles, except with monometallic CoCo-LDH enriched in Co^{2+} that displays active sites for H_2O_2 adsorption/reduction process.

2. Glucose detection

Electrochemical sensors and biosensors for glucose detection were first developed for diagnosis and monitoring of human diabetes [34]. Glucose plays also a major role in food products, such as juices. Hence, methods for detecting and quantifying glucose in assorted food matrices are also needed.

Several glucose biosensors based on the immobilization of glucose oxidase (GOx) in LDH host matrices have been described in the literature [2c, 8]. Indeed, LDHs display high adsorption capacities towards enzymes, such as GOx. Interactions between enzymes and LDH particles occur via electrostatic interactions. Owing to their large size, enzymes cannot be intercalated between LDH layers but they are adsorbed at the crystallite surface. GOx@LDH biosensors are mainly prepared as thin films coated on a Pt electrode by solvent casting. A drop of GOx/LDH aqueous mixture was deposited on the electrode and allowed to dry at low temperature. To limit enzyme leaching or improve the stability of the GOx@LDH/Pt films, subsequent cross-linking with glutaraldehyde can be applied or additives such as biopolymers (chitosan or alginate) can be used. In most cases, the transduction step corresponded to the electro-oxidation of the enzymatically generated H_2O_2 at the underlying Pt electrode. Recently, a new glucose amperometric biosensor has been prepared by a multilayer deposition on a GCE of CoMn-CO_3 LDH, GOx and a biopolymer (carrageenan), respectively [35]. The original transduction step consists in the electrocatalytic oxidation of enzymatically formed H_2O_2 in the CoMn-CO_3 inner-layer.

Besides these examples of GOx biosensors, several TM-LDHs have been described as good catalysts for glucose electro-oxidation. These are mainly nickel-based LDHs, Ni^{II}/Ni^{III} redox centers being involved in the following electrocatalytic reactions in alkaline electrolytes [36]:

$$Ni^{II}\text{-LDH} + OH^- \rightleftharpoons Ni^{III}(OH)\text{-LDH} + 1e^- \quad (3)$$

$$nNi^{III}(OH)\text{-LDH} + \text{glucose} \rightleftharpoons nNi^{II}\text{-LDH} + \text{oxidized glucose} \quad (4)$$

To our best knowledge, the nature of oxidized product formed during this electrocatalytic reaction is not identified. During the last two years, several strategies have been reported in the literature to improve the performance of these sensors, either by modifying the nature of trivalent cations associated with nickel (NiAl, NiFe, NiMn, NiCo), or by using electrode supports with a large surface area, such as carbon cloth (CC) or copper foam (CuF), to design porous 3D LDH nano-architectures providing interconnected channels to the active sites. Through some examples selected from the literature, we will illustrate these different approaches. Table 2 summarizes the performance of these selected Ni-based sensors for glucose determination which is generally realized in alkaline electrolytes (NaOH or KOH) at applied potentials ranging between 0.5 and 0.6 V.

Gualandi et al. [36] have optimized a glucose sensor with the electrosynthesis of NiAl-NO_3 on GCE, previously modified with carbon materials (RGO or MWCNTs). The presence of MWCNTs on the electrode surface improves the electrochemical performance of the glucose sensors by boosting the rate of electron transfer between the Ni catalytic centers and the GCE (Table 2). Similarly, carbon cloth (CC) provides a large surface area where 3D macroporous film of NiAl-LDH sheets can be prepared by an *in situ* growth technique [37]. The resulting electrode exhibits a high sensitivity toward glucose detection (14 A M^{-1} cm^{-2}). A similar strategy was adopted to prepare a 3D hierarchical structure based on NiFe-LDH [38]. In this case, cobalt carbonate hydroxide (CoCH) nanorods are preliminarily formed on the carbon cloth, to act as a guide support for the hydrothermal growth of NiFe-LDH nanosheets. Another 3D NiFe-LDH electrode was prepared by an electrodeposition process using Cu nanowires (CuNWs), grown on a Cu foam (CuF), as a firm grip for the NiFe-LDH nanosheets (Fig.4) [39].

Table 2 Electrochemical sensing of glucose using 3D Ni-based LDH modified electrodes

LDH	Electrode support	Sensing conditions	Sensitivity ($A\ M^{-1}\ cm^{-2}$)	LoD (μM)	Ref
NiAl	GCE RGO/GCE MWCNTs/GCE	E^{app} = 0.60 V/SCE 0.1 M NaOH	0.7 1.2 2.6	2 1 0.8	[36]
NiAl	CC	E^{app} = 0.66 V/Ag-AgCl 0.1 M NaOH 0.2	14	0.2	[37]
NiFe	CoCH/CC	E^{app} = 0.60 V/Hg-HgO 1 M KOH	6.6	3	[38]
NiFe	CuNWs/CuF	E^{app} = 0.40 V/Ag-AgCl 0.1 M KOH	7.9	0.1	[39]
NiMn	$NiCo_2O_4$/CC	E^{app} = 0.45 V/Hg-HgO 1.5 M KOH	2.1	0.2	[40]
NiCo	CC	E^{app} = 0.50 V/SCE 0.1 M KOH	5.0	0.12	[41]
	CoCuCH/CuF	E^{app} = 0.55 V/Ag-AgCl 0.2 M NaOH	10.8	0.68	[42]
	AuNPS/CuF	E^{app} = 0.50 V/Ag-AgCl 0.1 M NaOH	23.1	0.17	[43]
	CoxP/NiF	E^{app} = 0.64 V/Hg-HgO 0.1 M NaOH	5.7	0.6	[44]
	MOF-74(NiO)/CC	E^{app} = 0.55 V/Hg-HgO 1 M KOH	1.69	0.28	[45]
	MOF-NiCoS/CC	E^{app} = 0.50 V/Hg-HgO 0.5 M NaOH	2.16	0.21	[46]
	MOF- $NiFe_2O_4$/RGO/GCE	E^{app} = 0.50 V/SCE 0.1 M NaOH	0.11	13	[47]

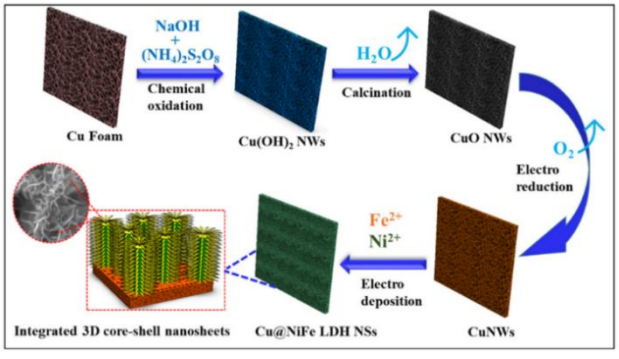

Fig. 4. Scheme of elaboration process of the NiFe-LDH/CuNWs/CuF electrode, Reprinted from [39] with permission from Elsevier

Even though these optimized 3D NiFe-LDH sensors demonstrated good sensitivity, they show worse performance than previously reported with NiAl-LDH/CC (Table 2). A 3D core–shell structure electrode (NiMn-LDH@$NiCo_2O_4$/CC) was successfully prepared by hydrothermal method. The $NiCo_2O_4$ nanowires, used as a core structure, provide stable electron transmission channels [40]. However, the performance of this modified electrode for glucose sensing (S = 2 A M^{-1} cm^{-2}) was not improved compared to the previously described sensors (Table 2).

As shown in Table 2, LDHs containing both nickel and cobalt (NiCo-LDH) appear to be the most efficient electrocatalysts for glucose sensing due to the electrocatalytic activity arising from both Ni^{II}/Ni^{III} and Co^{II}/Co^{III} redox couples. However, these LDHs exhibit a limitation in their electrocatalytic activity of sensors due to their low intrinsic conductivity and ease to aggregate. Several strategies have been described in the literature to build 3D nano-architectures based on NiCo-LDH on conductive supports to enhance the electrocatalytic properties and promote electronic and ionic transport in the electrodes (Table 2). Some of these strategies are very similar to the previously described for NiAl or NiFe-based LDH but leading to better performance, as illustrated below.

Wang et al. [41] have prepared ultrathin NiCo-LDH nanosheet array on carbon cloth by coprecipitation. This

sensor displayed a sensitivity of 5.12 A $M^{-1}cm^{-2}$ and a detection limit low as 0.12 µM, showing that NiCo-LDH can be a good candidate for enzymeless glucose sensing.

As previously shown with NiFe-LDH, cobalt carbonate hydroxide (CoCH) nanorods can be used as guiding template in LDH nanosheet growth. Moreover, copper foam seems to be an appropriate candidate as the conductive support since it possesses higher electrical conductivity than carbon cloth. Zhao et al. [42] have combined the NiCo-LDH structure with one-dimensional nanorods of cobalt copper carbonate hydroxide (CoCuCH) to form a core-shell structure on CuF. The sensitivity reported for this NiCo-LDH/CoCuCH/CuF electrode is better than that reported for the NiFe-LDH/CoCH/CC or NiFe-LDH/CuNWs/CuF (Table 2). A CuF was also decorated with AuNPs to be used as electrode support for the electrodeposition of NiCo-LDH nanoflake arrays (Fig.5) [43]. The 3D conductive structure composed of AuNPs and NiCo-LDH possesses higher electrical conductivity than NiCo-LDH/CuF electrode, and thus helps to improve the electron transfer in the LDH modified electrode. Owing to this synergistic effect, the 3D-architecture NiCo-LDH/AuNPs/CuF electrode exhibits an excellent electrocatalytic ability for glucose sensing in NaOH solution (S = 23 A M^{-1} cm^{-2}).

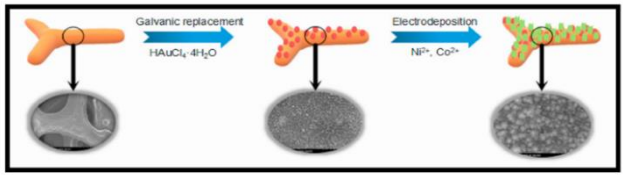

Fig. 5. Scheme of elaboration process of the NiCo-LDH/AuNPs/CuF electrode, Reprinted from [43] with permission from Elsevier.

Finally, 3D cobalt phosphide (CoxP) on NiF was used as a conductive support to synthesize a NiCo-LDH coating by electrogeneration [44]. Unfortunately, this heterostructure did not display any improvement in sensitivity (Table 2).

Metal organic frameworks (MOFs) can be used as a template to synthesize NiCo-LDH with novel hierarchical and submicroscopic structures leading to superior pseudocapacitance properties[48]. Wang et al. have adopted the same strategy for glucose sensing, via MOF-template methods to design 2D heterostructures of NiCo-LDH/NiO [45] or NiCo-LDH/NiCoS [46] grown on CC. Figure 6 shows the different steps for the preparation of the NiCo-LDH/NiO/CC electrode. First, 3D-flower-like MOF-74(Ni) was directly grown on the CC through a hydrothermal method, and then the as-prepared MOF-74(Ni)/CC was calcined to get nickel oxide (NiO). Finally, NiCo-LDH was formed on the NiO/CC electrode by a simple electrochemical deposition. The as-prepared NiCo-LDH/NiO/CC electrode displays an original flower-like structure compared to NiCo-LDH directly electrodeposited on CC, which has a neat and orderly nanosheet structure (Fig.6). Similarly, Chu et al. [47] have built a hollow-cube hierarchical structure based of NiCo-LDH/$NiFe_2O_4$/RGO using a cube-like NiFe bimetallic organic framework (NiFe-MOF) as template. This composite material deposited on GCE was also tested as a glucose electrochemical sensor. Unfortunately, these very sophisticated methods, via MOF templates do not provide any improvement in analytical performance for glucose determination (Table 2).

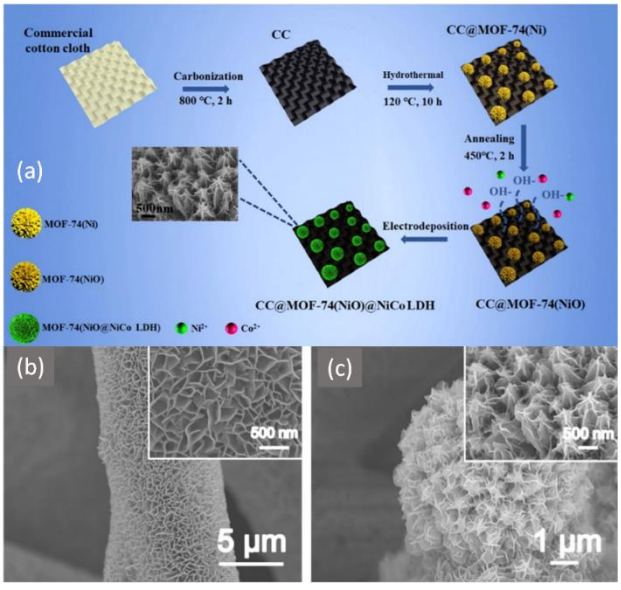

Fig. 6. Scheme of elaboration process of 3D multistage structure NiCo-LDH/MOF-74(NiO)/CC (a), SEM images of NiCo-LDH/CC (b) and NiCo-LDH/MOF-74(NiO)/CC (c) Reprinted from [45] with permission from Elsevier.

3. Glyphosate detection

As reported by Sohrabi et al. [16] LDHs are layered materials with special characteristics favorable for pesticide detection. Organophosphate, such as glyphosate (N(phosphonomethyl)glycine, Glyp) and glufosinate ((DL-homoalanine-4-yl)-methylphosphinic acid, Gluf), constitute one family of pesticides which was the most commonly used in agriculture. Due to the risks associated with aquatic contamination or human exposure to these pesticides, environmental monitoring of these pollutants require the development of selective and portable sensing methods [49]. In 2009, our group in Clermont-Ferrand was the first to describe an amperometric sensor based on a NiAl-NO_3/Pt modified electrode for the electrochemical

detection in one step of these herbicides[50]. NiAl-NO_3 films were formed on Pt electrodes by the electrodeposition method. As described for glucose, the electro-detection was based on the oxidation by Ni^{II}/Ni^{III} centers under alkaline condition of the amine group in the herbicide molecules. Under this pH condition (pH 13.0), the adsorption of these herbicides on LDH platelets remains very weak, but the electrocatalytic efficiency appears to be strongly dependent on the morphology of the NiAl-NO_3 film that may be controlled with the electrodeposition conditions. The electrochemical responses of the optimized NiAl-NO_3/Pt modified electrode were obtained by chronoamperometry at 0.49 V/SCE with a sensitivity of 287 mA M^{-1} cm^2 and a LoD of 1 µM for Glyp, the sensitivity found for Gluf was lower (178 mA M^{-1} cm^{-2}). Very recently, Zhao et al. [51] reported a new method to prepare NiAl-LDH electrode for glyphosate detection. A NiAl-LDH coating was prepared on Ni nanorods arrays (Ni-NRAs) by electrodeposition in the presence of Glyp in the electrolytic metal salts solution. This later molecule plays the role of template to form an inorganic-framework molecular imprinting material (NiAl-MI). Glyp molecule was removed from the NiAl-MI by a low temperature plasma treatment. The NiAl-MI/Ni-NRAs exhibited a rapid and high amperometric response at 0.37 V/Ag-AgCl toward successive Glyp additions in 1 M KOH electrolyte, leading to an excellent sensitivity of 705 A M^{-1} cm^{-2} and a low limit of detection (3 nM). The electrocatalytic oxidation ability at the NiAl-LDH interface is promoted by triggering the highly active Ni^{III} sites (and their induced OH* radicals) at relatively lower anodic potentials.

Finally, a nanocomposite CuAl-LDH@G casted on GCE was also reported as an electrochemical sensor for glyphosate detection. In 0.2 M acetate buffer solution (NaAc/HAc, pH 5.4), CuAl-LDH@G/GCE showed a well-defined oxidation peak at ≈ 0.1 V/Ag-AgCl, ascribed to the stripping redox process of copper from the LDH structure (Cu^I/Cu^{II}). In the presence of Glyp, that has a strong affinity for copper, a stable Cu-glyphosate complex may be formed leading to a decrease of the copper redox signal. The electrochemical detection of Glyp was performed under differential pulse voltammetry between 0.3 and -0.3 V, after an accumulation step of 180 s at -0.1 V/Ag-AgCl. In this case, the LoD was estimated at 1 nM, the sensitivity was not reported.

4. Conclusion

All these examples illustrate perfectly the potential of TM-LDHs in the design of electrochemical sensors. Even if the electrochemical mechanisms are not clearly established, we can draw some conclusions from this literature review. It appears that nickel-based LDHs show the most interesting electrocatalytic properties for the design of amperometric sensors. Thanks to the presence of iron or cobalt in the LDH hydroxide layers, an improvement of the electrocatalytic efficiency was observed towards the oxidation in alkaline medium of H_2O_2 with NiFe-LDH and glucose with NiCo-LDH, respectively. The use of supporting electrodes with a large specific surface area, such as carbon cloth or copper foam, modified with metallic nanoparticles (AuNPs or AgNPS) improves the electrical conductivity in the LDH modified electrodes and thus the electrochemical accessibility of the Ni sites. Moreover, these M-NPs can contribute with their own electrocatalytic properties, leading to an improvement of the analytical performance. Elaboration of porous nano-structures with Ni-LDHs nanosheets on these electrode surfaces allows a rapid diffusion of the analytes and a good accessibility of the active sites. However, more sophisticated hierarchical nano-structures built with TM-LDH, that are promising for supercapacitor applications, do not seem to be useful for sensor design. The wide range of possible compositions remains a major asset of LDHs. Insertion of other TMs, as illustrated with manganese or copper based-LDH, will certainly open new ways. We anticipate that this analysis will be useful for the design of new LDH-based electrochemical sensors, as illustrated with glyphosate.

Conflict of Interest

The authors declare no conflict of interest.

5. References

[1] aA. Walcarius, D. Mandler, J. A. Cox, M. Collinson, O. Lev, *J. Mater. Chem.* **2005**, *15*, 3663-3689. DOI.org/10.1039/B504839G ; bA. Walcarius, *Chem. Mater.* **2001**, *13*, 3351-3372. DOI.org/10.1021/cm0110167

[2] aZ. Navrartilova, P. Kula, *Electroanalysis* **2003**, *15*, 837-846. DOI.org/10.1002/elan.200390103 ; bC. Mousty, *Appl. Clay Sci.* **2004**, *27*, 159-177. doi.org/10.1016/j.clay.2004.06.005 ; cC. Mousty, *Anal. Bioanal. Chem.* **2010**, *396*, 315-325. DOI.org/10.1007/s00216-009-3274-y

[3] aD. Tonelli, E. Scavetta, M. Giorgetti, *Anal. Bioanal. Chem.* **2013**, *405*, 603-614. DOI.org/10.1007/s00216-012-6586-2 ; bC. Mousty, F. Leroux, *Recent Pat. Nanotechnol.* **2012**, *6*, 174-192. DOI.org/10.2174/187221012803531556

[4] N. Kajal, V. Singh, R. Gupta, S. Gautam, *Environ. Res.* **2022**, *204*, 112320. DOI.org/10.1016/j.envres.2021.112320

[5] aA. Walcarius, *Anal. Bioanal. Chem.* **2010**, *396*, 261-272. DOI.org/10.1007/s00216-009-3069-1 ; bA.

Walcarius, *Chem. Soc. Rev.* **2013**, *42*, 4098-4140. DOI.org/10.1039/C2CS35322A
[6] A. Kim, I. Varga, A. Adhikari, R. Patel, *Nanomater.* **2021**, *11*. DOI.org/10.3390/nano11112809
[7] C. Taviot-Guého, V. Prévot, C. Forano, G. Renaudin, C. Mousty, F. Leroux, *Adv. Funct. Mater.* **2018**, *28*, 1703868. DOI.org/10.1002/adfm.201703868
[8] C. Mousty, V. Prevot, *Anal. Bioanal. Chem.* **2013**, *405*, 3513-3523. DOI.org/10.1007/s00216-013-6797-1
[9] M.-Q. Zhao, Q. Zhang, J.-Q. Huang, F. Wei, *Adv. Funct. Mater.* **2012**, *22*, 675-694. DOI.org/10.1002/adfm.201102222
[10] Z. Zhang, P. Li, X. Zhang, C. Hu, Y. Li, B. Yu, N. Zeng, C. Lv, J. Song, M. Li, *Nanomater.* **2021**, *11*, 2644. DOI.org/10.3390/nano11102644
[11] C. Jing, B. Q. Dong, Y. X. Zhang, *Energy Environ. Mater.* **2020**, *3*, 346-379. DOI.org/10.1002/eem2.12116
[12] aG. Chen, H. Wan, W. Ma, N. Zhang, Y. Cao, X. Liu, J. Wang, R. Ma, *Adv. Energy Mater.* **2020**, *10*, 1902535. DOI.org/10.1002/aenm.201902535 ; bH. Yi, S. Y. Liu, C. Lai, G. M. Zeng, M. F. Li, X. G. Liu, B. S. Li, X. Q. Huo, L. Qin, L. Li, M. M. Zhang, Y. K. Fu, Z. W. An, L. Chen, *Adv. Energy Mater.* **2021**, *11*. DOI.org/10.1002/aenm.202002863
[13] D. Tonelli, I. Gualandi, E. Musella, E. Scavetta, *Nanomater.* **2021**, *11*. DOI.org/10.3390/nano11030725
[14] M. Asif, A. Aziz, M. Azeem, Z. Wang, G. Ashraf, F. Xiao, X. Chen, H. Liu, *Adv. Colloid Interface Sci.* **2018**, *262*, 21-38. DOI.org/10.1016/j.cis.2018.11.001
[15] H. Sohrabi, E. Dezhakam, A. Khataee, E. Nozohouri, M. R. Majidi, N. Mohseni, E. Trofimov, Y. Yoon, *Environ. Res.* **2022**, *211*, 113068. DOI.org/10.1016/j.envres.2022.113068
[16] H. Sohrabi, O. Arbabzadeh, M. Falaki, M. R. Majidi, N. Han, Y. Yoon, A. Khataee, *Food Chem. Toxicol.* **2022**, *164*, 113010. DOI.org/10.1016/j.fct.2022.113010
[17] H. Sohrabi, A. Khataee, S. Ghasemzadeh, M. R. Majidi, Y. Orooji, *Trends Environ. Anal. Chem.* **2021**, *31*, e00139. DOI.org/10.1016/j.teac.2021.e00139
[18] W. Chen, S. Cai, Q.-Q. Ren, W. Wen, Y.-D. Zhao, *Analyst* **2012**, *137*, 49-58. DOI.org/10.1039/C1AN15738H
[19] Y. Guo, X. Liu, X. Wang, A. Iqbal, C. Yang, W. Liu, W. Qin, *RSC Adv.* **2015**, *5*, 95495-95503. DOI.org/10.1039/C5RA18087B
[20] aL. Chen, B. Sun, X. Wang, F. Qiao, S. Ai, *J. Mater. Chem. B* **2013**, *1*, 2268-2274. DOI.org/10.1039/C3TB00044C ; bW. N. Yang, J. Li, M. Liu, D. H. L. Ng, Y. Liu, X. F. Sun, J. Yang, *Appl. Clay Sci.* **2019**, *181*, 12. DOI.org/10.1016/j.clay.2019.105238
[21] L. Su, X. N. Yu, W. J. Qin, W. P. Dong, C. K. Wu, Y. Zhang, G. J. Mao, S. L. Feng, *J. Mater. Chem. B* **2017**, *5*, 116-122. DOI.org/10.1039/c6tb02273a
[22] aT. Zhan, J. Kang, X. Li, L. Pan, G. Li, W. Hou, *Sens. Actuators, B* **2018**, *255*, 2635-2642. DOI.org/10.1016/j.snb.2017.09.074 ; bW. Shen, J. Sun, J. Y. H. Seah, L. Shi, S. Tang, H. K. Lee, *Anal. Chim. Acta* **2018**, *1001*, 32-39. DOI.org/10.1016/j.aca.2017.11.003
[23] aJ. Zhao, Y. Xie, W. Yuan, D. Li, S. Liu, B. Zheng, W. Hou, *J. Mater. Chem. B* **2013**, *1*, 1263-1269. DOI.org/10.1039/C2TB00389A ; bJ. X. Xie, W. J. Chen, X. X. Wu, Y. Y. Wu, H. Lin, *Anal. Methods* **2017**, *9*, 974-979. DOI.org10.1039/c6ay02731h
[24] Z. J. Yin, J. J. Wu, Z. S. Yang, *Biosens. Bioelectron.* **2011**, *26*, 1970-1974. DOI.org/10.1016/j.bios.2010.08.049
[25] aP. Vialat, F. Leroux, C. Mousty, *J. Solid State Electrochem.* **2015**, *19*, 1975-1983. DOI.org/10.1007/s10008-014-2671-0 ; bC. Taviot-Gueho, P. Vialat, F. Leroux, F. Razzaghi, H. Perrot, O. Sel, N. D. Jensen, U. G. Nielsen, S. Peulon, E. Elkaim, C. Mousty, *Chem. Mater.* **2016**, *28*, 7793-7806. DOI.org/10.1021/acs.chemmater.6b03061
[26] Y. Tao, Q. Chang, Q. Liu, G. Yang, H. Guan, G. Chen, C. Dong, *Surf. Interfaces* **2018**, *12*, 102-107. DOI.org/10.1016/j.surfin.2018.05.006
[27] H. Heli, J. Pishahang, H. B. Amiri, *J. Electroanal. Chem.* **2016**, *768*, 134-144. doi.org/10.1016/j.jelechem.2016.01.042
[28] H. Farhat, C. Taviot-Gueho, G. Monier, V. Briois, C. Forano, C. Mousty, *J. Phys. Chem. C* **2020**, *124*, 15585-15599. DOI.org/10.1021/acs.jpcc.0c03860
[29] L. Xu, M. L. Lian, X. Chen, Y. L. Lu, W. S. Yang, *Microchim. Acta* **2017**, *184*, 3989-3996. DOI.org/10.1007/s00604-017-2428-4
[30] Q. Chen, R. Ding, H. Liu, L. Zhou, Y. Wang, Y. Zhang, G. Fan, *ACS Appl Mater Interfaces* **2020**, *12*, 12919-12929. DOI.Org/10.1021/acsami.0c01315
[31] B. Habibi, F. F. Azhar, J. Fakkar, Z. Rezvani, *Anal. Methods* **2017**, *9*, 1956-1964. DOI.org/10.1039/C6AY03421G
[32] K. Zhang, H. Y. Zeng, M. X. Wang, Z. Li, *Ionics* **2022**, *28*, 5561-5570. DOI.org/10.1007/s11581-022-04777-z
[33] M. Asif, H. Liu, A. Aziz, H. Wang, Z. Wang, M. Ajmal, F. Xiao, H. Liu, *Biosens. Bioelectron.* **2017**, *97*, 352-359. doi.org/10.1016/j.bios.2017.05.057
[34] H. Teymourian, A. Barfidokht, J. Wang, *Chem. Soc. Rev.* **2020**, *49*, 7671-7709. DOI.org/10.1039/D0CS00304B
[35] H. Farhat, J. Célier, C. Forano, C. Mousty, *Electrochimica Acta* **2021**, *376*, 138050. https://doi.org/10.1016/j.electacta.2021.138050
[36] I. Gualandi, Y. Vlamidis, L. Mazzei, E. Musella, M. Giorgetti, M. Christian, V. Morandi, E. Scavetta, D. Tonelli, *ACS Appl. Nano Mater.* **2019**, *2*, 143-155. DOI.org/10.1021/acsanm.8b01765
[37] B. Hai, Y. Zou, *Sens. Actuators, B* **2015**, *208*, 143-150. DOI.org/10.1016/j.snb.2014.11.022
[38] D. Song, L. L. Wang, B. Wang, J. G. Yu, Y. T. Li, Y. N. Qu, C. P. Duan, Y. Y. Yang, X. L. Miao, *Int. J. Electrochem. Sci.* **2020**, *15*, 1949-1963. DOI.Org/10.20964/2020.03.04
[39] N. Rafique, A. H. Asif, R. A. K. Hirani, H. Wu, L. Shi, S. Zhang, H. Q. Sun, *J. Colloid Interface Sci.* **2022**, *615*, 865-875. DOI.org/10.1016/j.jcis.2022.02.037
[40] J. H. Li, L. L. Wang, Y. Y. Yang, B. Wang, C. P. Duan, L. L. Zheng, R. L. Li, Y. J. Wei, J. Q. Xu, Z. Yin, *Nanotechnology* **2021**, *32*. DOI.Org/10.1088/1361-6528/ac2764
[41] X. Wang, Y. Zheng, J. Yuan, J. Shen, J. Hu, A.-J. Wang, L. Wu, L. Niu, *Electrochim. Acta* **2017**, *224*, 628-635. DOI.org/10.1016/j.electacta.2016.12.104
[42] Z. T. Zhao, Y. J. Sun, J. X. Song, Y. J. Li, Y. Xie, H. Cui, W. P. Gong, J. Hu, Y. Chen, *Sens. Actuators, B* **2021**, *326*. DOI.org/10.1016/j.snb.2020.128811
[43] M. Shen, W. Li, L. Chen, Y. X. Chen, S. B. Ren, D. M. Han, *Anal. Chim. Acta* **2021**, *1177*. DOI.org/10.1016/j.aca.2021.338787

[44] Y. Zhang, Z. Y. He, Q. Y. Dong, X. Tang, L. Yang, K. Huang, Z. R. Zou, X. Jiang, X. L. Xiong, *Microchem. J.* **2022**, *172*. DOI.org/10.1016/j.microc.2021.106923

[45] L. L. Wang, Y. Y. Yang, B. Wang, C. P. Duan, J. H. Li, L. L. Zheng, J. H. Li, Z. Yin, *J. Alloys Compd.* **2021**, *885*. DOI.org/10.1016/j.jallcom.2021.160899

[46] L. L. Wang, J. H. Li, Y. B. Zhao, H. J. He, L. L. Zheng, Z. J. Huang, X. Zhao, J. Q. Xu, B. Wang, Z. Yin, *Mater. Adv.* **2022**, *3*, 6028-6036. DOI.Org/10.1039/d2ma00454b

[47] D. W. Chu, F. B. Li, X. M. Song, H. Y. Ma, L. C. Tan, H. J. Pang, X. M. Wang, D. X. Guo, B. X. Xiao, *J. Colloid Interface Sci.* **2020**, *568*, 130-138. DOI.org/10.1016/j.jcis.2020.02.012

[48] Z. Jiang, Z. Li, Z. Qin, H. Sun, X. Jiao, D. Chen, *Nanoscale* **2013**, *5*, 11770-11775. 10.1039/C3NR03829G

[49] K. Zúñiga, G. Rebollar, M. Avelar, J. Campos-Terán, E. Torres, *Water* **2022**, *14*, 2436. DOI.org/10.3390/w14152436

[50] A. Khenifi, Z. Derriche, C. Forano, V. Prevot, C. Mousty, E. Scavetta, B. Ballarin, L. Guadagnini, D. Tonelli, *Anal. Chim. Acta* **2009**, *654*, 97-102. DOI.org/10.1016/j.aca.2009.09.023

[51] Y. G. Zhao, Y. Yan, C. Y. Liu, D. T. Zhang, D. Wang, A. Ispas, A. Bund, B. Du, Z. D. Zhang, P. Schaaf, X. Y. Wang, *ACS Appl. Mater. Interfaces* **2022**, *14*, 35704-35715. DOI.org/10.1021/acsami.2c0850035704